First-Principles Study for the Anisotropy of Iron-based Superconductors toward Power and Device Applications

Hiroki Nakamura,[1,2,3] Masahiko Machida,[1,2,3] Tomio Koyama,[4,3] and Noriaki Hamada[5]

[1]*CCSE, Japan Atomic Energy Agency, 6–9–3 Higashi-Ueno, Taito-ku Tokyo 110–0015, Japan*
[2]*JST, Transformative Research-Project on Iron Pnictides (TRIP), Chiyoda, Tokyo 102-0075, Japan*
[3]*CREST (JST), 4–1–8 Honcho, Kawaguchi, Saitama 332–0012, Japan*
[4]*Institute for Materials Research, Tohoku University, 2-1-1 Katahira, Aoba-ku, Sendai 980-8577, Japan*
[5]*Faculty of Science and Technology, Tokyo University of Science, 2641 Yamazaki, Noda 278-8510, Japan*

(Dated: October 1, 2009)

Performing the first-principles calculations, we investigate the anisotropy in the superconducting state of iron-based superconductors to gain an insight into their potential applications. The anisotropy ratio γ_λ of the c-axis penetration depth to the ab-plane one is relatively small in $BaFe_2As_2$ and LiFeAs, i.e., $\gamma_\lambda \sim 3$, indicating that the transport applications are promising in these superconductors. On the other hand, in those having perovskite type blocking layers such as $Sr_2ScFePO_3$ we find a very large value, $\gamma_\lambda \gtrsim 200$, comparable to that in strongly anisotropic high-T_c cuprate $Bi_2Sr_2CaCu_2O_{8-\delta}$. Thus, the intrinsic Josephson junction stacks are expected to be formed along the c-axis, and novel Josephson effects due to the multi-gap nature are also suggested in these superconductors.

PACS numbers: 74.25.Jb,74.70.-b,71.15.Mb

Since the discovery of iron-based superconductor $LaFeAsO_{1-x}F_x$ with T_c = 26K by Kamihara *et al.*[1], high-T_c superconductivity has been reported in some of its family materials. All the superconductors in this family have FePn layers (Pn = P, As, or Se), in which the high-T_c superconductivity emerges, and are classified into five groups according to the non-superconducting blocking layers sandwiched between FePn layers as seen in Fig. 1, i.e., 1111 (e.g., LaFeAsO), 122 (e.g., $BaFe_2As_2$)[2], 111(e.g., LiFeAs)[3], 11(e.g., FeSe)[4], and the other type that contains very thick perovskite-based blocking layers ($Sr_2ScFePO_3$)[5].

The quasi two-dimensionality of the electronic states due to the layer structure of the iron-based superconductors is significant for their applications, since it causes anisotropy in superconducting properties such as the critical current J_c and the upper and lower critical fields, H_{c2} and H_{c1}. A convenient quantity characterizing the superconducting anisotropy is the anisotropy parameter γ_λ defined as the ratio of the c-axis penetration depth to the in-plane one. From the values of γ_λ, one can extract important information about their potential applications. For example, superconductors with small γ_λ are suitable for power applications using superconducting wires, tapes or cables. On the other hand, those with extremely large γ_λ are expected to work as the intrinsic Josephson junctions [6, 7], which will be promising as a THz emission device [8, 9].

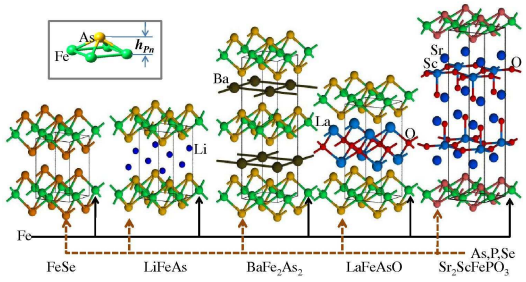

FIG. 1: Crystal structures of typical iron-based superconductors.

It is well known that the penetration depth anisotropy γ_λ directly leads to the anisotropy of H_{c2}, H_{c1} and J_c in single-band superconductors. In the multi-band systems such as the iron-based superconductors their relations become much more complicated and are still controversial [10]. But, in any case the parameter γ_λ describes the scale of the superconducting anisotropy. Thus, in this paper we perform a systematic first-principles study for γ_λ in the whole groups of iron-based superconductors and elucidate the origin of the general trend in the superconducting anisotropy observed in various measurements such as torque, microwave surface impedance, J_c, etc. [11, 12, 13, 14, 15, 16, 17, 18, 19, 20, 21]. Though accurate values of γ_λ have not yet been settled experimentally, i.e., the reported values are still scattered, we find a clear trend in γ_λ among the five groups of the iron-based superconductors. Moreover, since we can predict the anisotropy ratio of a superconductor in which single crystals are not available, our method presented in this paper will provide a powerful tool for the exploration of the superconducting materials suitable for each application. Our calculations reveal that the anisotropy ratio γ_λ depends sensitively on the nature of the blocking layers and its values are widely distributed as seen in experiments, e.g., $\gamma_\lambda \sim 3$ in the superconductors belonging

TABLE I: Lattice constants a and c, the height $h_{\rm Pn}$ of As, P , or Se ions from the Fe-plane, and the anisotropy parameters of the resistivity and the penetration depth at zero temperature. a, c, and $h_{\rm Pn}$ are experimental values as the input parameters for the first-principles calculations, and γ_ρ and γ_λ are the calculated ones.

	a[Å]	c[Å]	$h_{\rm Pn}$[Å]	$\gamma_\rho(0)$	$\gamma_\lambda(0)$
FeSe	3.7738	5.5248	1.4652	18.44	4.29
LiFeAs	3.7914	6.3639	1.6769	9.06	3.01
$BaFe_2As_2$	3.9625	13.0168	1.3602	10.69	3.27
LaFePO	3.9636	8.5122	1.1398	17.34	4.16
LaFeAsO	4.020	8.7034	1.3238	116.8	10.81
$Sr_2ScFePO_3$	4.016	15.543	1.1984	6.19×10^5	248

to the 111 and 122 groups and $\gamma_\lambda \gtrsim 200$ in those with perovskite-based blocking layers. These results remind us of the variety in high-T_c cuprates, e.g., $\gamma_\lambda \sim 8$ in $YBa_2Cu_3O_{8-\delta}$ and $\gamma_\lambda > 100$ in $Bi_2Sr_2CaCu_2O_{8-\delta}$(Bi-2212) [22]. It is noted that the anisotropy in the 111 and 122 groups is small in spite of the layer structure. The large value of γ_λ in the group with perovskite-based blocking layers strongly suggests the formation of the intrinsic Josephson junction stacks along the c-axis.

In this paper, we evaluate γ_λ for the typical iron-based superconductors from numerical results for the anisotropy ratio of the normal state resistivity at $T = 0$K, $\gamma_\rho(0)$ obtained by means of the first-principles calculations for the electronic states [23], that is, the superconducting anisotropy originating from the band-structure dependent Fermi velocities is considered. Let us first summarize the method employed in this paper to evaluate the anisotropy parameters, γ_ρ and γ_λ. Assuming that the relaxation time of the conduction electrons is isotropic and independent of their velocities, we consider the quantity $\gamma_\rho(0) = \langle v_a^2\rangle_{\rm FS}/\langle v_c^2\rangle_{\rm FS}$ to be equal to the ratio of the c-axis resistivity to the a-axis one. Here, v_a and v_c are the Fermi velocities, respectively, parallel and perpendicular to the FePn layers and $\langle\cdots\rangle_{\rm FS}$ denotes the average on the Fermi surface [23]. The Fermi velocities are derived from the derivative of the band energy, $v_i = \partial\epsilon_k/\partial k_i$, where the band energy ϵ_k is calculated by the first-principles calculations. In our calculations we use the first-principles density functional package VASP[24], which adopts GGA exchange-correlation energy [25] and PAW method [26]. The electron self-consistent loops to obtain the charge density are repeated until the total energy difference becomes smaller than 10^{-6} eV. In these loops the spacing between nearest-neighbor k-points is taken to be ~ 0.1–0.2 Å^{-1}. Once the charge density is determined, the energy bands are again calculated for more k-points located with a much finer spacing, 79×79, in the xy-plane (the number of k-points along the z-axis depends on the compounds), in order to determine the Fermi surfaces and the Fermi velocities.

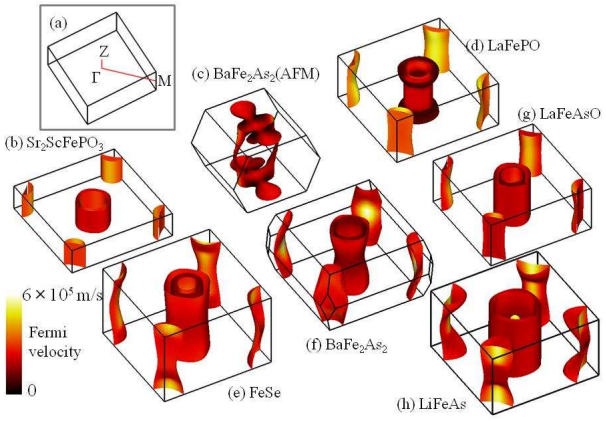

FIG. 2: The Fermi surfaces of (b) $Sr_2ScFePO_3$, (c) antiferromagnetic $BaFe_2As_2$, (d) LaFePO, (e) FeSe, (f) $BaFe_2As_2$, (g) LaFeAsO, and (h) LiFeAs. The contrast on the surfaces indicates the magnitude of the Fermi velocity. The inset (a) shows typical symmetry points.

The average $\langle\cdots\rangle_{\rm FS}$ is calculated by the standard tetrahedron method. In obtaining the anisotropy of the penetration depth at zero temperature, we utilize the simplest relation, $\gamma_\lambda(0) = \sqrt{\gamma_\rho(0)}$ [27], which is convenient for systematic and comparative studies on the superconducting anisotropy among various iron-based superconductors, though its validity is limited in the multi-band systems[27]. The compounds that we examine in this paper are FeSe, LaFeAsO, LaFePO, $BaFe_2As_2$, LiFeAs, and $Sr_2ScFePO_3$. The calculations are done for tetragonal undoped compounds without any magnetic order, except for $BaFe_2As_2$. We calculate the electronic structures based on the observed crystalline structures, that is, the crystalline structures are not optimized, since it is known that the optimized structure deviates from the observed one in iron-based superconductors. [5, 28, 29, 30, 31, 32].

The numerical results for the anisotropy parameters, γ_ρ and γ_λ, in the iron-based superconductors employed in this paper are summarized in Table I. Let us discuss the 1111-system, first. The experimental values in this group are widely distributed, depending on the compounds [11, 13, 14, 15, 16, 19, 20, 21]. For example, $\gamma_\lambda \sim 15-20$ in ReFeAsO (Re=Nd, Sm) [11, 15, 21], while $\gamma_\lambda \sim 3$ in PrFeAsO [20]. Thus, we notice that there are two groups in the 1111-system, i.e., the one with relatively large anisotropy and the other with moderate anisotropy. In our calculations, we obtained $\gamma_\lambda(0) = 10.81$ for LaFeAsO, as shown in Table I. This value is close to that in the group with relatively large anisotropy. We also performed the calculations for stoichiometric PrFeAsO and obtained $\gamma_\lambda(0) \sim 8.6$, which is smaller than that in LaFeAsO as expected and also not far from the observed one in $PrFeAsO_{1-y}$. This difference between LaFeAsO and PrFeAsO can be mainly attributed to the difference of the main elements inside the blocking layers. On the

other hand, it is also noted that the calculated value in non-arsenic 1111-compound LaFePO ($\gamma_\lambda(0) = 4.16$) is much smaller than that of LaFeAsO, though the crystal structures are equivalent in both compounds. The Fermi surface shapes are different in these two compounds as seen in Figure 2 (d) and (g), that is, the Fermi surfaces in LaFeAsO are almost cylindrical, while those in LaFePO are not, indicating that the two-dimensionality is weak in LaFePO. From these results, one understands that the two-dimensionality differs among the 1111 compounds even if the blocking layers are equivalent. This remarkable feature comes from the fact that the band dispersion along the z-direction is sensitively related to the Pn's height from the Fe's square lattice plane. It is also noticed that the anisotropy of the 1111 compounds ($\gamma_\lambda \gtrsim 10$) is on the same order as in $YB_2Cu_3O_{8-\delta}$, that is, the transport application will be promising in the 1111-compounds.

In the 122-compound $BaFe_2As_2$, we obtained $\gamma_\lambda(0) = 3.27$. This value is smaller than that of LaFeAsO (1111-system) and is consistent with the experimental one ~ 6 [11], which is generally smaller than that in the 1111-system. The weak anisotropy in the 122-compound is also understood from the feature of the Fermi surfaces. As seen in Fig.2, the Fermi surfaces in this compound are more winding along the z-direction compared with that in LaFeAsO, which leads to the weak anisotropy in the superconducting state of the 122-compounds. This indicate that the 122 system has high potential for transport applications. The 122-compound makes a tetragonal-to-orthorhombic transition, and a stripe-type antiferromagnetic (AFM) order appears in the low temperature phase. We also calculated the anisotropy parameter γ_ρ in the antiferromagnetic phase ($\mu_{\rm Fe} = 1.9\mu_{\rm B}$) [33] and found $\gamma_\rho(0) = 1.2$, which is smaller than that of the tetragonal one being consistent with the experiments. In fact, the experimental value is $\gamma_\rho \sim 2.5$ [12]. Thus, one finds that the anisotropy becomes weaker in the AFM phase. Note that the reduction in the resistivity anisotropy originates from the three-dimensional Fermi surfaces appearing in the AFM phase as seen in Fig.2(c). These results clearly demonstrate the advantage of the present evaluation technique. In Table I we also list the anisotropy parameters of LiFeAs in the 111-system. The γ_λ value is comparable to $BaFe_2As_2$, that is, the 111-system is also suitable for transport applications. This low anisotropy basically reflects the winding features of the Fermi surface like 122-systems as seen in Fig.2(h).

In the 11-compounds FeSe, which has the simplest crystal structure composed of a stack of only FePn layers, the Fermi surfaces calculated in this compound shows clear curvature along the z-direction as seen in Fig.2(e), indicating that the two-dimensionality is weak in this system. In fact, we obtained a relatively small value, $\gamma_\lambda(0) = 4.29$, in the superconducting state. However, we note that this value is larger than those in the 122 and 111 systems and rather close to that in LaFePO. From this result one understands that metallic ions in the blocking layers enhance the three dimensionality in the 122 and 111 systems. We emphasize that only the first-principles calculations can systematically derive such delicate material-dependent difference in the anisotropy.

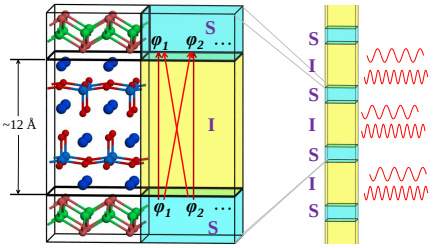

FIG. 3: A schematic illustration of the intrinsic Josephson junction stacks in $Sr_2ScFePO_3$. An alternate stack of FePn (superconducting) and blocking layers (insulating) are regarded as a series of S-I-S Josephson junctions. φ_i stands for the phase of the superconducting order-parameter of the ith electron energy band. The arrows represent possible tunneling channels.

Now, we discuss the anisotropy in the final group, i.e., the newly discovered iron-based superconductors with perovskite-type blocking layers, which are now under intensive exploration. The superconductors in this group do not show any magnetic order at all, while the superconducting transition temperature is rather high. In this paper we focus on a typical compound, $Sr_2ScFePO_3$, which shows the highest T_c at ambient pressure among non-arsenic iron-based superconductors. Since the blocking layers in this compound are very thick as shown in Fig.1, strong anisotropy is expected in the normal state resistivity. In fact, a huge value $\gamma_\rho \sim 10^6$ is obtained, which is several hundred times larger than that in the other groups,i.e., 1111-, 122-, and 11- compounds. From this normal state value it follows, $\gamma_\lambda(0) \sim 250$, for the anisotropy in the London penetration depth of $Sr_2ScFePO_3$. Note that the value is comparable to that in Bi-2212 in high-T_c cuprates. From this fact one may infer that the c-axis transport in this system is brought about by the electron tunneling between neighboring FePn layers, as in Bi-2212. In the superconducting state the Cooper-pair tunneling will be also expected to occur between the superconducting FePn layers as in Bi-2212, that is, a single crystal of $Sr_2ScFePO_3$ may be regarded as a stack of nano-scale Josephson junctions as schematically shown in Fig.3, which is called the intrinsic Josephson junctions. In the intrinsic Josephson junctions the $I-V$ characteristics under no external magnetic field show a remarkable feature, i.e., the *multiple branch structure* composed of many $I-V$ curves [6], the number of which corresponds to that of stacked intrinsic SIS junctions as shown in Fig.3. Hence, we naturally expect that the multiple-branch structure appears in the c-axis

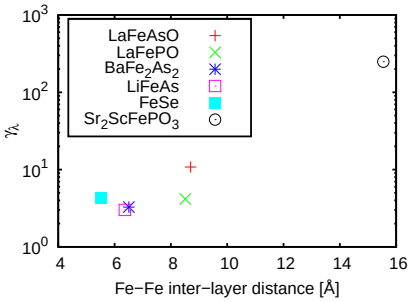

FIG. 4: The penetration-depth anisotropy as a function of the distance between Fe-planes.

$I-V$ characteristics in the superconducting state in a single crystal of $Sr_2ScFePO_3$. As for the damping nature in the Josephson effects, this system should be underdamped one, because the paring symmetry is expected to be mainly full gapped s-wave one. It is also predicted that a new oscillation mode exists in the phase differences in addition to the Josephson plasma [34]. Moreover, the Josephson vortex has an internal structure [35]. These new features originates from the multi-tunneling channels due to the multi-gap nature in these superconductors as shown in Fig.3. The existence of the new phase oscillation modes will enrich the physics in the intrinsic Josephson junctions expected in the new compounds. We also mention that the superconducting $Sr_2ScFePO_3$ is a stoichiometric compound, that is, the superconductivity appears without doping. Then, it will be easier to make a stack of homogeneous intrinsic Josephson junctions in a large-scale, which is contrasted with the Bi-2212 intrinsic Josephson junctions, in which the doping for getting the high-T_c superconductivity brings about disorders.

Finally, we summarize our numerical results for γ_λ vs. distance between adjacent iron-planes in Fig.4. From this figure one finds a rough trend between the distance and the anisotropy, which indicates that the anisotropy increases with increasing the distance. However, our results also suggests the existence of the other factors that affect the penetration depth anisotropy. As discussed in this paper, the anisotropy is sensitive to the distance between the pnictogen ions and the Fe-plane, and also the elements forming the blocking layers. From these results we claim that the method presented in this paper, using the first-principles calculations, is a powerful tool for evaluating the superconducting anisotropy.

In summary, we investigated systematically the anisotropy of the London penetration depth for various iron-based superconductors on the basis of the first-principles calculations for their electronic states. It was shown that the anisotropy parameters, γ_ρ and γ_λ, are strongly dependent on the structure of the blocking layers and pnictogen ions situated next to Fe layers. Our numerical results well explain the variety of the γ_λ values observed in these superconductors. The 122- and the 111-compounds show weak anisotropy, being enough for transport power applications, while those with perovskite-type blocking layers have a very large value of γ_λ, which is comparable to that in Bi-2212. We predict that the intrinsic Josephson junction stacks are realized in the superconducting state of these compounds.

The authors wish to thank H. Ogino and J. Shimoyama for providing their recent experimental results and K. Terakura for illuminating discussion in first-principles calculations. The authors also thank N. Hayashi, Y. Nagai, M. Okumura, and N. Nakai for valuable discussion. The work was partially supported by Grant-in-Aid for Scientific Research on Priority Area "Physics of new quantum phases in superclean materials" (Grant No. 20029019) from the Ministry of Education, Culture, Sports, Science and Technology of Japan.

[1] Y. Kamihara *et al.*, J. Am. Chem. Soc. **130**, 3296 (2008).
[2] M. Rotter, M. Tegel, and D. Johrendt, Phys. Rev. Lett. **101**, 107006 (2008); K. Sasmal *et al.*, Phys. Rev. Lett. **101**, 107007 (2008).
[3] J.H. Tapp *et al.*, Phys. Rev. B **78**, 060505 (2008).
[4] F.-C. Hsu *et al.*, Proc. Natl. Acad. Sci. USA 105, 14262 (2008).
[5] H. Ogino *et al.*, Supercond. Sci. Technol. 22, 075008 (2009).
[6] R. Kleiner *et al.*, Phys. Rev. Lett. 68, 2394 (1992).
[7] G. Oya *et al.*, Jpn. J. Appl. Phys. 31, L829 (1992).
[8] L. Ozyuzer *et. al.*, Science 318, 1291 (2007).
[9] K. Kadowaki *et. al.*, Physica C 468, 634 (2008).
[10] V.G. Kogan, Phys. Rev. Lett. **89**, 237005 (2002).
[11] R. Prozorov *et al.*, Physica C 469, 582 (2009).
[12] M. A. Tanatar *et al.*, Phys. Rev. B 79, 134528 (2009).
[13] D. Kubota *et al.*, arXiv:0810.5623.
[14] S. Weyeneth *et al.*, J. Supercond. Nov. Magn. 22, 325 (2009).
[15] S. Weyeneth *et al.*, J. Supercond. Nov. Magn. 22, 347 (2009).
[16] J. Jaroszynski *et al.*, Phys. Rev. B 78, 174523 (2008).
[17] M. Kano *et al.*, arXiv:0904.1418.
[18] Z. Bukowski *et al.*, Phys. Rev. B 79, 104521 (2009).
[19] Y. Jia *et al.*, Supercond. Sci. Technol. 21, 105018 (2008).
[20] R. Okazaki *et al.*, Phys. Rev. B 79,064520 (2009).
[21] C. Martin *et al.*, Phys. Rev. Lett. 102, 247002 (2009).
[22] See e.g., J. C. Martinez *at al.*, Phys. Rev. Lett. **69**, 2276 (1992), and references therein.
[23] N. Hamada, T. Imai, H. Funashima, J. Phys.:Condens. Matter **19**, 365221 (2007).
[24] G. Kresse and J. Hafner, Phys. Rev. B **47**, RC558 (1993); G. Kresse and J. Furthmüller, Phys. Rev. B **54**, 11169 (1996).
[25] J. P. Perdew, K. Burke, M. Ernzerhof, Phys. Rev. Lett. **77** (1996) 3865.
[26] P. E. Blöchl, Phys. Rev. B **50**, 17953 (1994); G. Kresse and D. Joubert, Phys. Rev. B **59**, 1758 (1999).
[27] V.G. Kogan, Phys. Rev. B**66**, 020509(R) (2002).
[28] S. Margadonna *et al.*, Chem. Commun. 2008, 5607 (2008).

[29] J.H. Tapp *et al.*, Phys. Rev. B 78,060505(R) (2008).
[30] M. Rotter *et al.*, Phys. Rev. B 78, 020503 (2008).
[31] Y. Kamihara *et al.*, J. Am. Chem. Soc. **128**, 10012 (2006).
[32] C. de la Cruz *et al.*, Nature **453**, 899 (2008).
[33] The calculated moment becomes larger than the observed one. This is a well-known problem in first-principles calculations for iron-based superconductors. We avoid further discussion on this discrepancy. See e.g., [36] for its more details.
[34] Y. Ota *et al.*, Phys. Rev. Lett. 102, 237003 (2009).
[35] Y. Ota *et al.*, arXiv:0907.0277.
[36] I. I. Mazin, M. D. Johannes, L. Boeri, K. Koepernik, and D. J. Singh, Phys. Rev. B 78, 085104 (2008).